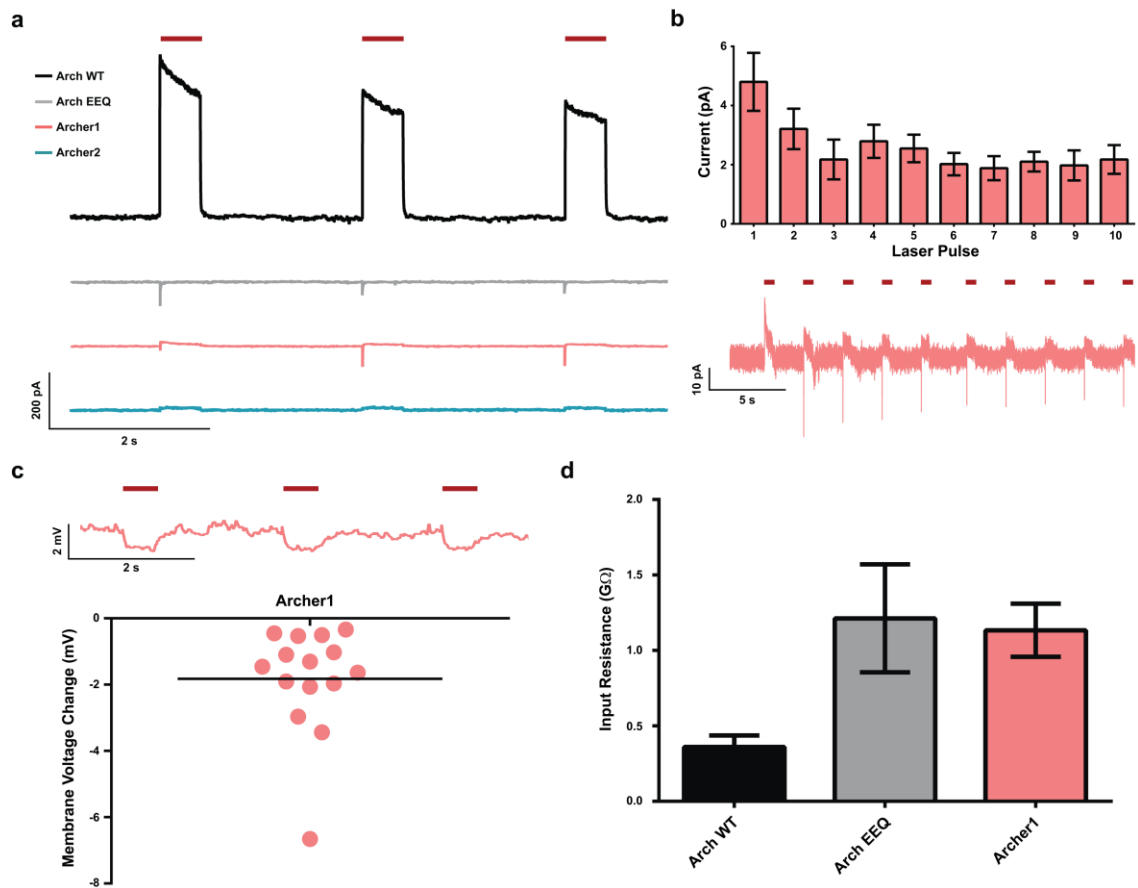


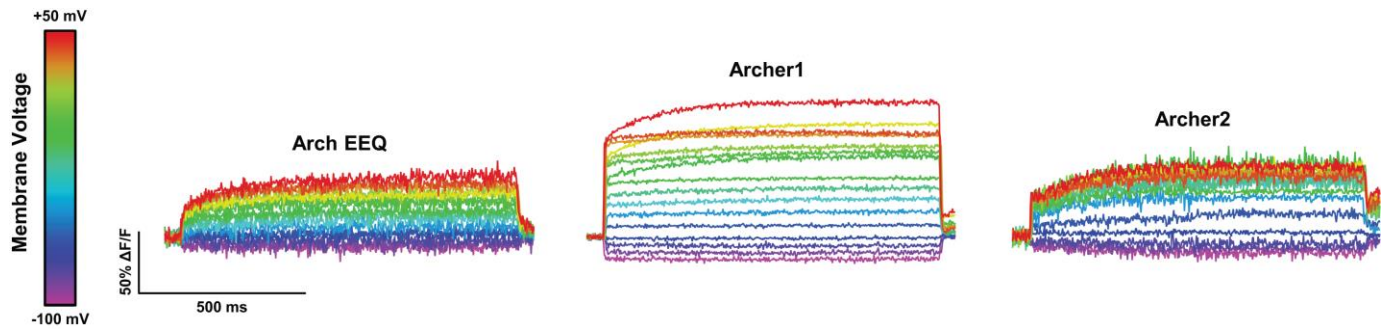
Supplementary Figure 1. Structural alignment of Arch variants with Arch-1

(a) Sequence alignment via ClustalW2. Arch-1¹ (Uniprot P69051), Archer1, and Archer2 share 93% amino acid identity. The alignment shows the D95E, T99C, and A225M mutations of Archer1 and Archer2 from Arch WT boxed in blue. (b) Archer1 construct design and schematic of location of opsin-fluorescent protein fusion in membrane. Locations of the mutated residues (D95 and T99) are shown in blue and their relative positions to the retinal chromophore in black.



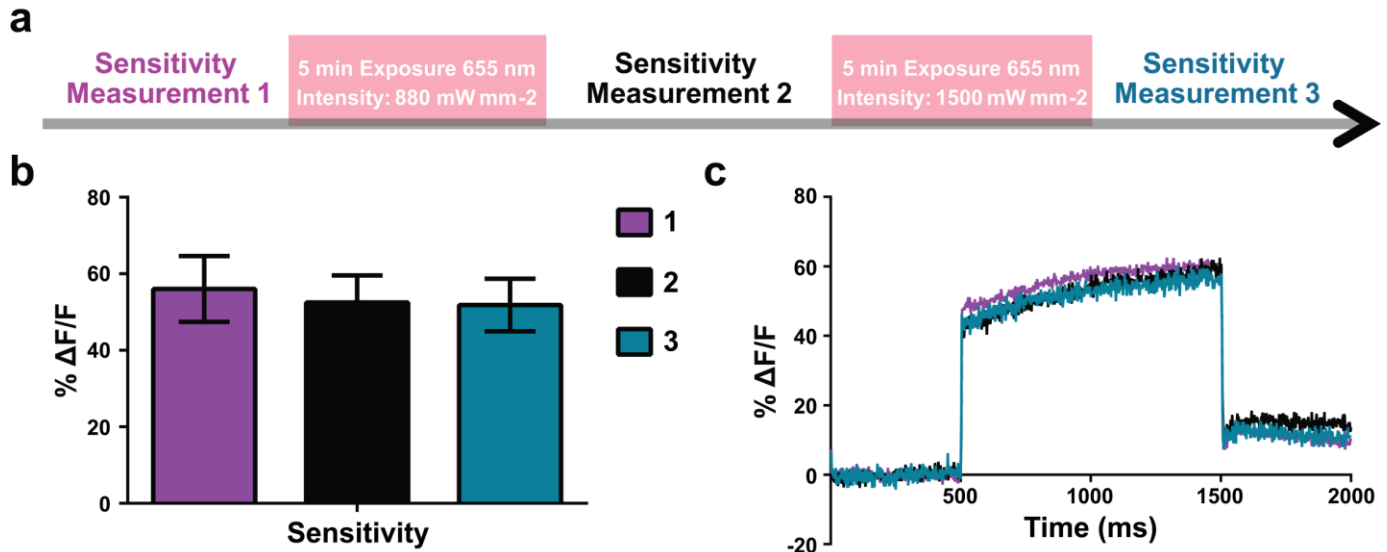
Supplementary Figure 2. Residual photocurrents of Arch variants and effect on membrane potential

(a) Single trace voltage-clamp recordings of photocurrents in neurons expressing Arch WT and variants in response to three consecutive pulses of laser illumination at the intensity used for fluorescence imaging. Arch EEQ, as previously reported, shows no steady-state photocurrent in response to laser illumination, while Archer1 and Archer2 exhibit small steady-state currents. Arch EEQ and Archer1 both respond to laser illumination with a brief peak of depolarizing photocurrent before reaching steady state. This has been observed with microbial rhodopsin-based voltage sensors as previously reported for Mac². (b) Archer1 photocurrent characteristics are measured in response to 10 consecutive laser pulses ($n = 10$). An initial peak current is generated in naïve cells exposed to laser illumination for the first time. Subsequent pulses reach a lower steady state without a peak. (c) Current clamp recordings of changes in membrane voltage of neurons expressing Archer1 ($n = 15$) induced by pulses of laser illumination. (d) Input resistance of patched cells expressing Arch WT ($n = 8$), Arch EEQ ($n = 10$), and Archer1 ($n = 10$) recorded as a measure of quality of the seal break. Laser illumination for Arch WT, Archer1, and Archer2 ($\lambda = 655 \text{ nm}$; $I = 880 \text{ mW mm}^{-2}$), and Arch EEQ ($\lambda = 655 \text{ nm}$; $I = 1,500 \text{ mW mm}^{-2}$). Error bars represent standard error of the mean (s.e.m.).



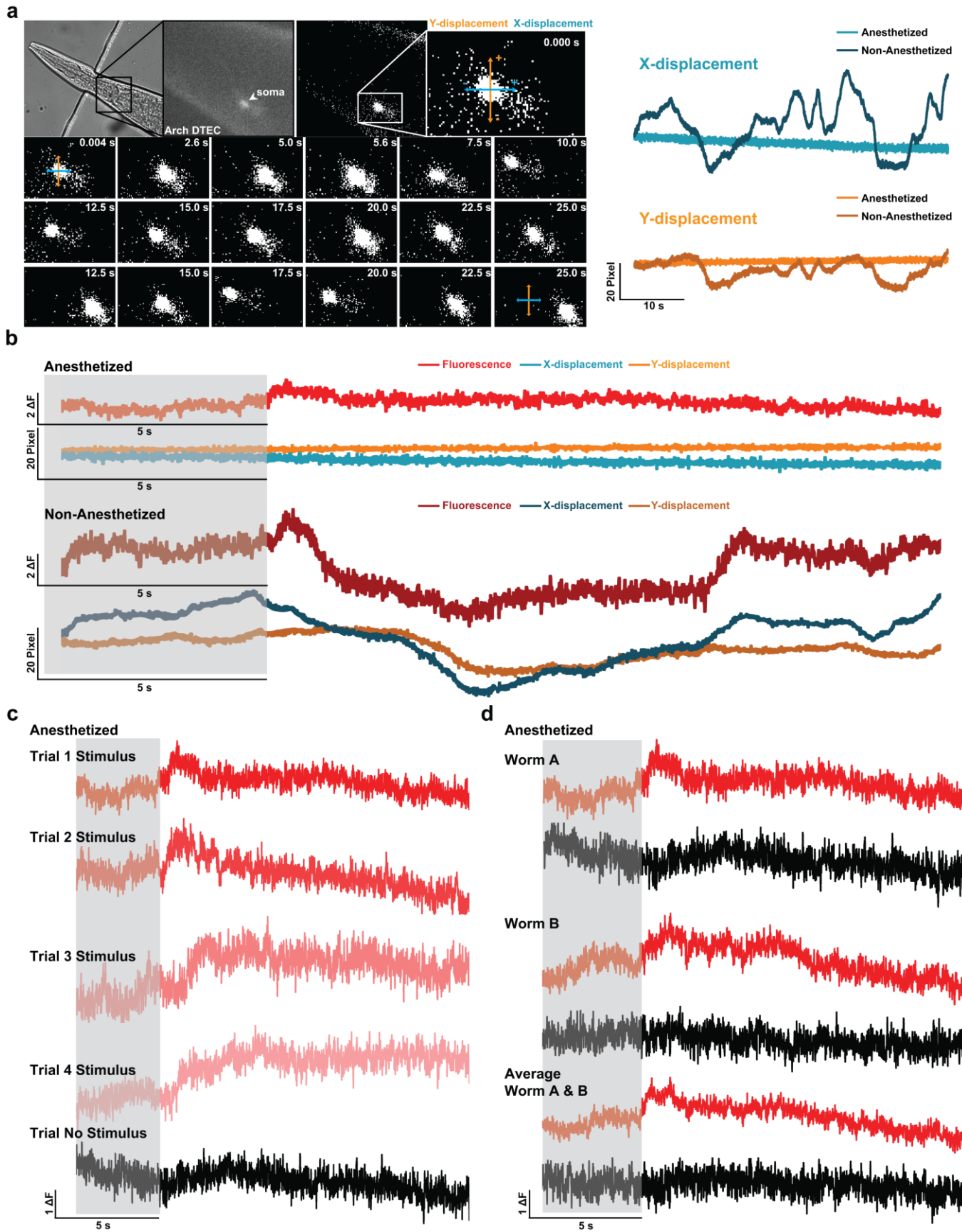
Supplementary Figure 3. Averaged fluorescence sensitivity of Arch variants

Averaged fluorescence responses (imaged at 500 Hz) of neurons expressing Arch EEQ ($n = 5$), Archer1 ($n = 10$), and Archer2 ($n = 3$) to voltage clamped steps in membrane potential. Neurons are held at -70 mV and then stepped to voltages ranging from -100 mV to +50 mV in increments of 10 mV. Laser illumination for Archer1 and Archer2 ($\lambda = 655 \text{ nm}$; $I = 880 \text{ mW mm}^{-2}$), and Arch EEQ ($\lambda = 655 \text{ nm}$; $I = 1,500 \text{ mW mm}^{-2}$).



Supplementary Figure 4. Archer1 fluorescence sensitivity is stable with prolonged illumination

(a) Laser exposure and sensitivity measurement paradigm consists of detecting the sensitivity of fluorescence response to 100 mV voltage step in three consecutive measurements separated by 5 minutes of continuous laser exposures, with the first exposure at 880 mW mm⁻² and the second at 1,500 mW mm⁻². (b) The average percentage change in fluorescence in response to 100 mV step in voltage does not significantly change after the first ($n = 8$) or second ($n = 6$) prolonged laser exposure. (c) Average fluorescence waveforms for the sensitivity measurements described in (a, b) show no change in the characteristics of fluorescence response. Laser illumination for Archer1 ($\lambda = 655$ nm; $I = 880$ mW mm⁻²). Error bars represent standard error of the mean (s.e.m.).



Supplementary Figure 5. Worm movement and fluorescence in anesthetized vs. non-anesthetized worms

(a) Tracking fluorescence of an AWC cell throughout a stimulus paradigm. Cell location is determined by averaging coordinates of fluorescent pixels above a set threshold and monitoring their position on an x-y coordinate plane over time. Non-anesthetized worms show significant movement in both x (blue) and y (red) direction throughout the stimulation protocol compared to anesthetized worms. (b) Changes in fluorescence in response to cessation of exposure to odorant stimulus (IAA) are time-locked to respective cell movement for anesthetized vs. non-anesthetized worms. Non-anesthetized worms show frequent changes in fluorescence correlated with movement, not apparent in anesthetized worms. (c) Fluorescence traces of repeated trials of stimulation (red) within the same worm compared to control (black). (d) Single trial fluorescence response to stimulus and control paradigms for two worms (A and B) and the average fluorescence trace of the two. Fluorescence traces imaged at $\lambda = 655 \text{ nm}$; $I = 880 \text{ mW mm}^{-2}$. Fluorescence traces (ΔF) in (b)-(d) have undergone background subtraction and Gaussian averaging.

Supplementary Table 1. Accession codes

Construct	Addgene #
pLenti-CaMKIIa-eArch3.0-EYFP	35514
FCK-Arch-GFP	22217
pLenti-Arch-EEQ	45188

Supplementary Table 2. Cloning primers

Primer	Sequence	Used for
Archfwd	CCGGATCCGCCACCATGGACC	Forward primer for Arch amplification
ERrev	GGGAATTCTCATTACACCTCGTTCTCGTAGC	Reverse primer for Arch amplification
Arch3.0_D95E_T99C_fwd	GCCGAGTGGCTGTTTTGCACCCC	Insertion of D95E and T99C mutations into Arch
Arch3.0_D95E_T99C_rev	GGTGCAAAACAGCCACTCGGCGTAC	Insertion of D95E and T99C mutations into Arch
Arch3.0_A225M_fwd	TTATGGTGTGGACGTGACTATGAAGGTCGG	Insertion of A225M mutation into Arch
Arch3.0_A225M_rev	AGTCACGTCCAACACCATAACAGCAGAG	Insertion of A225M mutation into Arch
TSrev_into_GFPstart	AGCTCCTCGCCCTTGCTCACCACGTTGATGTCGATCTGG TCCAGGG	Used for amplification and assembly of Arch-TS with EGFP-ERexport
GFPfwd_overlapTSEND	ACCAGATCGACATCAACGTGGTGAGCAAGGGCGAGGAG CTG	Amplification of GFP out of FCK-Arch-GFP
FCK-GFPprev_ERexport	CCGAATTCTTACACCTCGTTCTCGTAGCAGAACTTGTAC AGCTCGTCCATGCCGAGAG	Amplification of GFP out of FCK-Arch-GFP and addition of ERexport domain
str-2p-SphI-F2(2K)	CGGGGCATGCGTGGGTAGTTTATGTTGCAATCATCAG	Amplification of <i>str-2</i> AWC specific promoter
str-2p-Ascl-R2	GGCGGGCGCGCCTTTTATGGATCACGAGTATTCGGACA A	Amplification of <i>str-2</i> AWC

		specific promoter
Arch-NheI-AAA-F	CTTAGCTAGCAAAATGGACCCCATCGCTCTGCA	Amplification and insertion of Archer1eGFP into pSM vector
Arch-EcoRI-R	ATTGGAATTCTTACACCTCGTTCTCGTAGCAGAACTTGTA CAGCT	Amplification and insertion of Archer1eGFP into pSM vector

Supplementary References

- 1 Enami, N. *et al.* Crystal structures of archaerhodopsin-1 and -2: Common structural motif in archaeal light-driven proton pumps. *Journal of molecular biology* **358**, 675-685, doi:10.1016/j.jmb.2006.02.032 (2006).
- 2 Gong, Y., Wagner, M. J., Zhong Li, J. & Schnitzer, M. J. Imaging neural spiking in brain tissue using FRET-opsin protein voltage sensors. *Nat Commun* **5**, 3674, doi:10.1038/ncomms4674 (2014).